Analysis of Artificial Dielectrics Composed of Non-Aligned Layers

Daniele Cavallo[1] and Cantika Felita[1]
[1]Microelectronics dept., Delft University of Technology, Delft, The Netherlands, d.cavallo@tudelft.nl

***Abstract*—In this work, we present an analysis of artificial dielectric layers (ADLs), when a lateral shift between layers is present. The alternate lateral displacement of the layers is an important parameter to engineer the desired effective electromagnetic properties of the ADL material. More specifically, much higher equivalent dielectric constants can be realized by alternatively shifting the layers, compared to the aligned case. Closed-form expressions are given for the equivalent layer reactance that include the higher-order interaction between shifted layers. These analytical formulas are of great aid to design artificial dielectric slabs, as they provide the scattering parameters for generic plane-wave incidence. The effective permittivity and permeability tensors of the artificial dielectrics can then be retrieved from the scattering parameters.**

***Index Terms*—Artificial dielectric, scattering from grids.**

I. Introduction

ARTIFICIAL dielectrics (ADs) were introduced in [1] as a light-weight alternative to real dielectric materials, for realizing microwave lenses [2]. After their introduction, ADs have been extensively studied and used for decades for radar development. An AD consists of a large-scale model of an actual dielectric, obtained by embedding conducting structures in a host material according to a regular pattern. The electric field scattered by the metallic inclusions, when added to the incident field, creates an effective equivalent delay [3]. At the frequencies for which the periodicity of the pattern is much smaller than the wavelength, the structure can be assigned equivalent parameters that describe a homogeneous dielectric. The effective electric parameters can be engineered by varying the size of the metal obstacles and their spatial density. This work relates to a specific type of anisotropic ADs, which are realized as a cascade of planar layers made of printed metal patches, as depicted in Fig. 1. Such structures are also referred to as artificial dielectric layers (ADLs).

Recently, ADLs have been employed as superstrates to improve the radiation performance of planar antennas, both in the microwave [4] and in the terahertz [5] frequency range. In these works, ADLs were exploited to improve the front-to-back ratio of integrated antennas without supporting surface waves, with a consequent enhancement of gain and efficiency.

Closed-form expressions to describe the scattering from artificial dielectric slabs were derived in [6], [7]. These formulas account for the higher-order interaction between layers, which cannot be neglected due to the electrically small inter-layer distance. However, while [7] only contemplates the case of aligned layers (arranged as in Fig. 1), in this work we

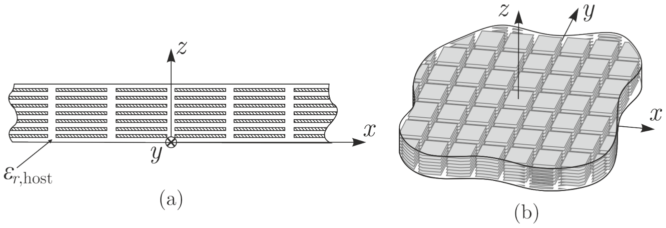

Fig. 1. Artificial dielectric slab with aligned layers: (a) two-dimensional side view; (b) three-dimensional prospective view.

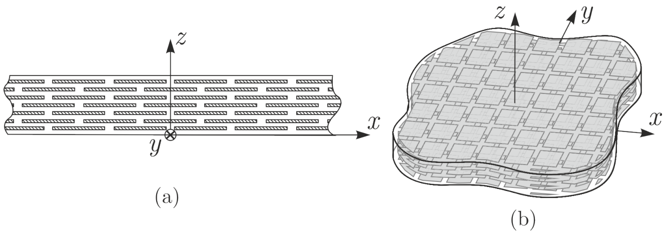

Fig. 2. Artificial dielectric slab with layers alternatively shifted in both x and y: (a) two-dimensional side view; (b) three-dimensional prospective view.

generalize the analysis to include the effects of alternate shifts, as shown in Fig. 2. This new configuration is very relevant for the design of ADLs, because the shift significantly increases the effective permittivity of the slab with respect to the aligned case. Consequently, the shift between layers represents an additional important degree of freedom that can be used for the design, as it greatly extends the ranges of permittivity values that can be synthesized, given a specific fabrication technology.

II. Analysis of Shifted ADLs

Let us consider an ADL medium composed by an infinite number of layers spaced along z by distance d_z and numbered with consecutive integer indexes n_z, as shown in Fig. 3(a). The odd layers ($n_z = [... - 3, -1, 1, 3, ...]$) are shifted with respect to the even layers ($n_z = [..., -2, 0, 2, ...]$) by s_x and s_y along x and y, respectively, as depicted in Fig. 3(b). We assume that a plane wave is traveling in the negative-z direction within the ADL medium, with electric and magnetic field indicated by $\mathbf{e}_i(x, y, z)$ and $\mathbf{h}_i(x, y, z)$, respectively (Fig. 4). By applying the equivalence theorem as in [7], we can define three surfaces S_1, S_0 and S_{-1} as in Fig. 5(a) and denote with '1' and '2' the two regions above and below the layer located at $z = 0$. The

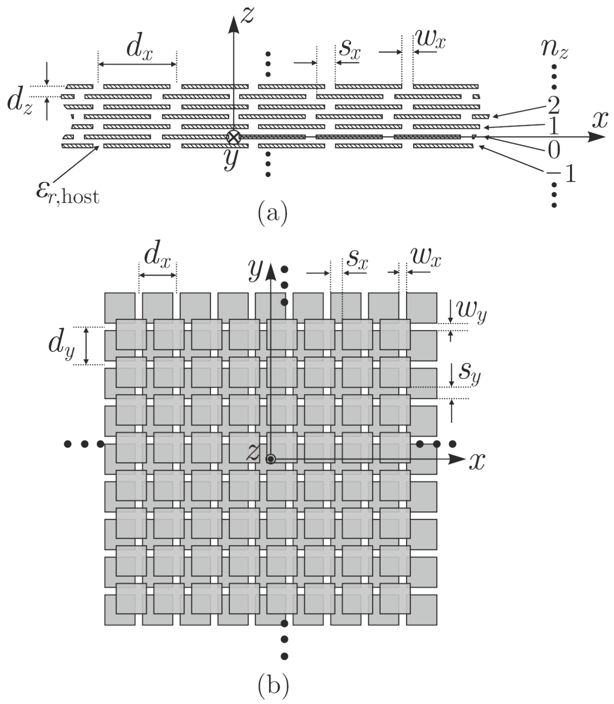

Fig. 3. Definition of the geometrical parameters characteristic of the shifted ADLs: (a) cross section and (b) top view.

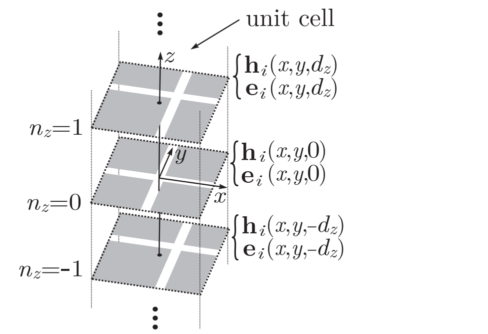

Fig. 4. Aperture fields on three layers of an infinite cascade of ADLs.

volume bounded by the surfaces can be filled with perfectly electric conductor (P.E.C.), as shown in Fig. 5(b), according to the Schelkunoff's version of the equivalence principle [8], so that only equivalent surface magnetic currents $\mathbf{m}_{n_z}(x,y)$ are present in correspondence of the gaps between patches in the initial problem.

The magnetic currents are related to the aperture electric field as

$$\mathbf{m}_{n_z}(x,y)|_{z=n_z d_z \pm \epsilon} = \mp \hat{\mathbf{z}} \times \mathbf{e}_i(x,y,z=n_z d_z \pm \epsilon) \qquad (1)$$

with ϵ being a vanishingly small distance. It is evident from (1) that the two magnetic current distributions above and below the layer $n_z = 0$ are equal and opposite to satisfy the continuity of the tangential electric field in the gap.

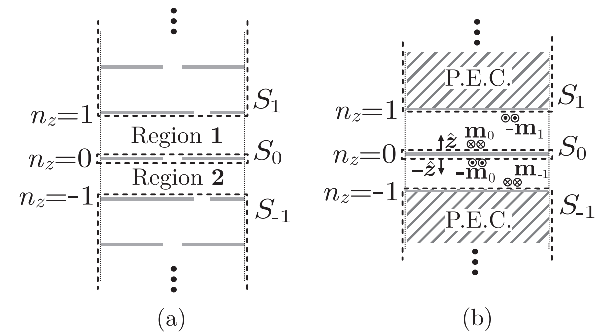

Fig. 5. (a) Definition of the surfaces for the equivalence principle and (b) equivalent problem with unknown magnetic current distributions.

A. Approximation on the Magnetic Current Distribution

Due to the periodicity along z, we can impose Floquet boundary conditions, i.e. the magnetic currents on the layers at $n_z = 1$ and $n_z = -1$ are related by a phase shift:

$$\mathbf{m}_1(x,y) = \mathbf{m}_{-1}(x,y) e^{jk_{zs} 2d_z} \qquad (2)$$

where k_{zs} is an unknown equivalent wavenumber describing the propagation along z. Since the periodic cell is a combination of two layers, we cannot relate the magnetic currents $\mathbf{m}_0$ and $\mathbf{m}_1$ using Floquet boundary condition. However, for the sake of simplicity of the formulation, we assume that the magnetic currents on the two layers are approximately equal in amplitude and differ only from a spatial displacement and a phase term:

$$\mathbf{m}_1(x,y) \approx \mathbf{m}_0(x-s_x, y-s_y) e^{-j\mathbf{k}_{\rho s}\cdot \mathbf{s}} e^{jk_{zs}d_z} \qquad (3)$$

$$\mathbf{m}_{-1}(x,y) \approx \mathbf{m}_0(x-s_x, y-s_y) e^{-j\mathbf{k}_{\rho s}\cdot \mathbf{s}} e^{-jk_{zs}d_z} \qquad (4)$$

where $\mathbf{k}_{\rho s} = k_{xs}\hat{\mathbf{x}} + k_{ys}\hat{\mathbf{y}}$, k_{xs} and k_{ys} are wavenumbers describing the propagation along x and y, respectively, and $\mathbf{s} = s_x\hat{\mathbf{x}} + s_y\hat{\mathbf{y}}$ is the vector indicating the shift. The approximation in (3) and (4) is equivalent to implying that the the field propagation from one layer to the next is dominated by a lossless guided phenomenon.

B. Integral Equation and Equivalent Reactance of the Layer

Under the assumption for the magnetic currents given by (3) and (4), and fixing $s_x = s_y$ to obtain azimuth-independent properties of the ADLs, we can generalize the method in [7] to account for the shift between the layers. The integral equation to be solved is derived by imposing the continuity of the total aperture magnetic field across the gaps between regions 1 and 2. By applying the image theorem, an infinite number of images of the magnetic currents are obtained, as described in Fig. 6. Similarly to [7], the difference between the total

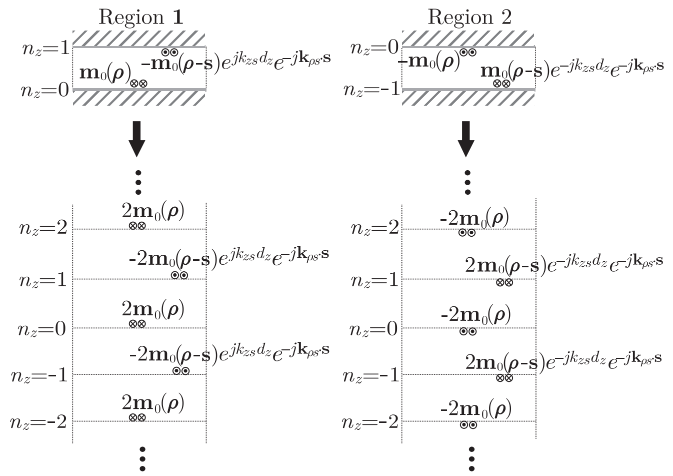

Fig. 6. Application of the image theorem for the two regions above and below the layer at $z = 0$ ($\boldsymbol{\rho} = x\hat{\mathbf{x}} + y\hat{\mathbf{y}}$).

fields in region 1 and region 2 can be written as

$$\sum_{n_z \text{even}} \iint_{-\infty}^{\infty} 4\mathbf{m}_0(\boldsymbol{\rho}')\mathbf{g}(\boldsymbol{\rho}-\boldsymbol{\rho}', n_z d_z, z=0)d\boldsymbol{\rho}' -$$
$$\sum_{n_z \text{odd}} \iint_{-\infty}^{\infty} 2(e^{jk_{zs}d_z} + e^{-jk_{zs}d_z})\mathbf{m}_0(\boldsymbol{\rho}'-\mathbf{s})\mathbf{g}(\boldsymbol{\rho}-\boldsymbol{\rho}', n_z d_z, z=0)$$
$$e^{-j\mathbf{k}_{\rho s}\cdot\mathbf{s}} d\boldsymbol{\rho}' = 2\mathbf{h}_i(\boldsymbol{\rho}, z=0) \quad (5)$$

where $\boldsymbol{\rho} = x\hat{\mathbf{x}} + y\hat{\mathbf{y}}$ and $\boldsymbol{\rho}' = x'\hat{\mathbf{x}} + y'\hat{\mathbf{y}}$ refer to the observation and the source points, respectively. The function g represents the free-space dyadic Green's function which relates the magnetic field to a magnetic source.

In the low-frequency limit, one can approximate the exponential terms with 1 (since $k_{zs}d_z \ll 1$ and $\mathbf{k}_{\rho s}\cdot\mathbf{s} \ll 1$), which leads to

$$\sum_{n_z \text{even}} \iint_{-\infty}^{\infty} 4\mathbf{m}_0(\boldsymbol{\rho}')\mathbf{g}(\boldsymbol{\rho}-\boldsymbol{\rho}', n_z d_z, 0)d\boldsymbol{\rho}' -$$
$$\sum_{n_z \text{odd}} \iint_{-\infty}^{\infty} 4\mathbf{m}_0(\boldsymbol{\rho}'-\mathbf{s})\mathbf{g}(\boldsymbol{\rho}-\boldsymbol{\rho}', n_z d_z, 0)d\boldsymbol{\rho}' \approx 2\mathbf{h}_i(\boldsymbol{\rho}, 0). \quad (6)$$

The approximated integral equation can now be solved in the spectral domain with a procedure similar to the one described in [7], thus omitted here. The only difference is that the spectral summations of Floquet waves are evaluated in closed-form separately for the two sets of even and odd layers. The procedure yields the following expression of the layer susceptance in the presence of the shift:

$$B_{s\infty} = \frac{j2k_0}{\zeta_0} \sum_{m_y \neq 0} \frac{|\text{sinc}(k_{ym}w_x/2)|^2}{|k_{ym}|} \cdot \left(-\cot(k_{zm}d_z) + e^{-jk_{ym}s_y}\csc(k_{zm}d_z)\right) \quad (7)$$

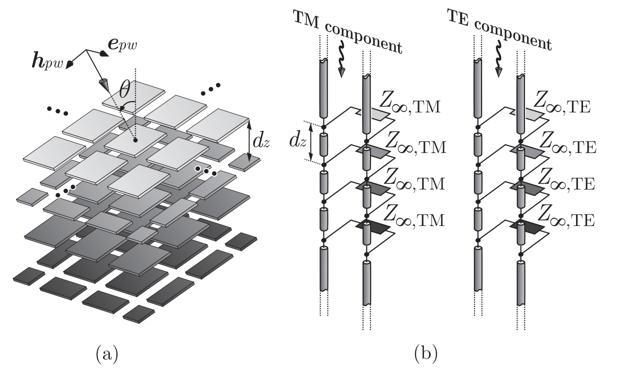

Fig. 7. (a) Plane wave impinging on a cascade of four ADLs with alternate shifts and (b) equivalent circuits for TE and TM components.

where $k_{zm} \approx -j|k_{ym}|$ and $k_{ym} \approx (-2\pi m_y)/d_y$ is the Floquet mode of index m_y. The analytical expression in (7) accounts for the higher-order coupling between layers and thus remains valid even for inter-layer distances much smaller than the wavelength. Analogously to [6], [7], one can express the reactance of a layer embedded in a periodic multi-layer environment as follows:

$$Z_{\infty,\text{TM}} = \frac{-j}{B_{s\infty}}, \quad Z_{\infty,\text{TE}} = \frac{-j}{B_{s\infty}(1-\frac{\sin^2\theta}{2})}. \quad (8)$$

III. Validation of the Analytical Formulas and Discussion

A. Equivalent Circuit

The values of the equivalent reactance, obtained for TE and TM incidence in (8), can be used within an equivalent circuit that describes the propagation of a generic plane wave in the ADL medium. The equivalent transmission lines are shown in Fig. 7(b) for the TE and TM components. To validate the formulas and assess the accuracy of the approximations we show in Fig. 8 the reflection and transmission coefficients for TE and TM plane-wave incidence (at $\theta = 60°$) and for different shifts. CST simulations [9] are also reported for the same structures and show good agreement with our method.

B. Retrieval of the Effective Parameters

From the scattering parameters calculated using the equivalent circuit in Fig. 7(b), one can retrieve the effective permittivity and permeability, using the formalism introduced in [10]. Since the ADL is an anisotropic material, the equivalent medium is characterized by permittivity and permeability tensors

$$\underline{\underline{\varepsilon}} = \varepsilon_0 \begin{pmatrix} \varepsilon_x & 0 & 0 \\ 0 & \varepsilon_y & 0 \\ 0 & 0 & \varepsilon_z \end{pmatrix}, \underline{\underline{\mu}} = \mu_0 \begin{pmatrix} \mu_x & 0 & 0 \\ 0 & \mu_y & 0 \\ 0 & 0 & \mu_z \end{pmatrix}. \quad (9)$$

When $s_x = s_y$, because of the square symmetry of the geometry, the condition $\varepsilon_x = \varepsilon_y$ is satisfied and the material is uniaxial. It is also evident that, for ADLs hosted in vacuum, we obtain $\varepsilon_z = 1$, because the z-component of the electric

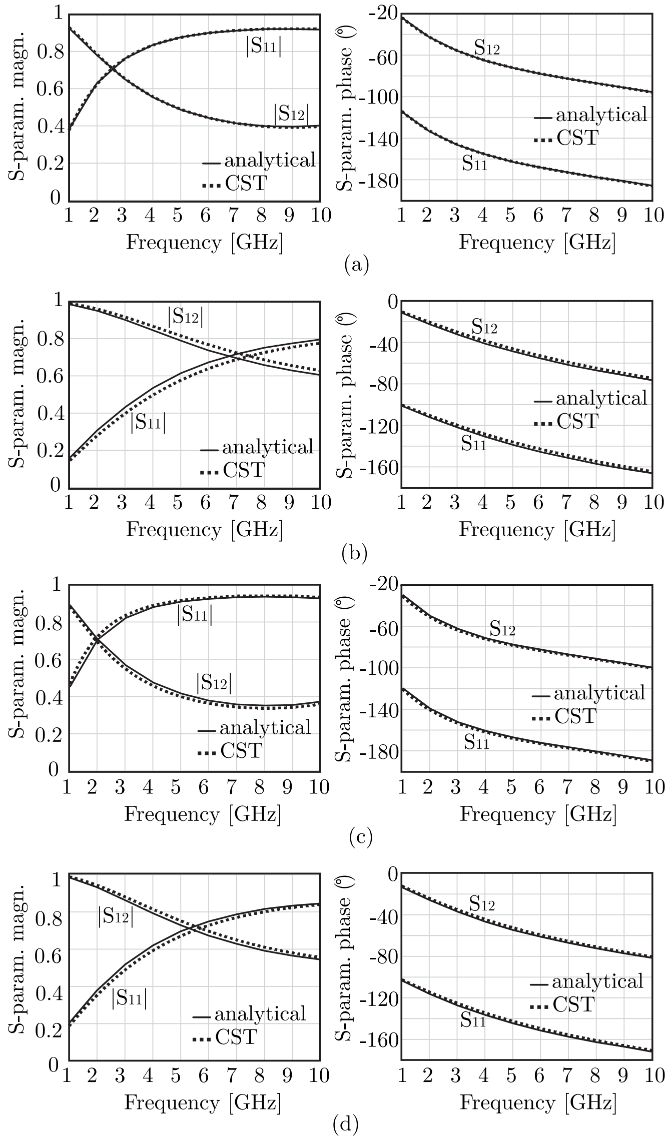

Fig. 8. Amplitude and phase of the reflection and transmission coefficients of a plane wave incident on a cascade of 5 layers: (a) TE, $\theta = 60°$, $s_{x,y} = 0.25d_{x,y}$; (b) TM, $\theta = 60°$, $s_{x,y} = 0.25d_{x,y}$; (c) TE, $\theta = 60°$, $s_{x,y} = 0.5d_{x,y}$; (d) TM, $\theta = 60°$, $s_{x,y} = 0.5d_{x,y}$. The geometrical parameters are $d_x = d_y = 0.0785\lambda_0$, $w_x = w_y = 0.01\lambda_0$, $d_z = 0.012\lambda_0$, with λ_0 being the wavelength at 5 GHz.

field does not interact with the horizontal patches. Strong diamagnetic effects are also occurring in the case of TE incidence, for which the magnetic field has a non-zero z-component. Indeed, in this case, the patches support loop currents that produce a magnetic field opposite to the incident one. Therefore, the total magnetic field inside the ADL is reduced compared to the external one (i.e., $\mu_z < 1$). The other components of the permeability tensors are $\mu_x = \mu_y = 1$. The variation of the ε_x and μ_z as a function of the shift is reported in Fig. 9. It can be noted that the permittivity components ε_x and ε_y increase with the shift, because of the raised mutual capacitance between layers. An opposite behavior is observed

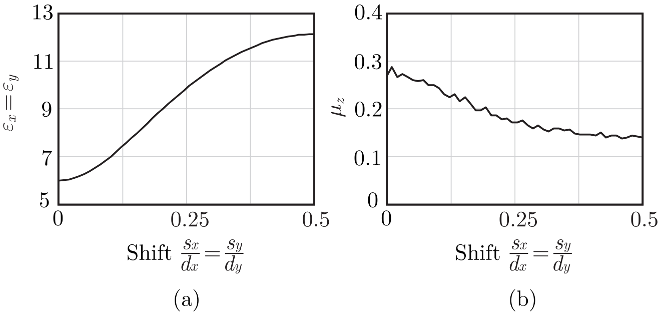

Fig. 9. (a) Equivalent x- and y- components of the relative permittivity tensor and (b) equivalent z-component of the relative permeability tensor, as a function of the shift. The ADL is composed of 5 layers embedded in a medium with $\varepsilon_{r,\text{host}} = 1$, with $d_x = d_y = 0.0785\lambda_0$, $w_x = w_y = 0.01\lambda_0$, $d_z = 0.012\lambda_0$, with λ_0 being the wavelength at the calculation frequency.

for the permeability component μ_z, which decreases as a function of the shift.

IV. Conclusions

We derived closed-form formulas for the analysis of artificial dielectric layers (ADLs). The expressions of the equivalent reactance of each layer include the effect of an arbitrary shift between odd and even layers. The higher-order interaction between layers is rigorously accounted for in analytical form. The reactances can be embedded in an equivalent circuit that provides the scattering parameters for generic plane-wave incidence and for an arbitrary number of layers. The results given by our method were validated with simulations performed with commercial electromagnetic solvers. From the scattering parameters, the permittivity and permeability tensors can also be derived.

References

[1] W. E. Kock, "Metallic delay lenses," *Bell System Tech. J.*, vol. 27, no. 1, pp. 58-82, Jan. 1948.

[2] S. S. D. Jones and J. Brown, "Metallic delay lenses," *Nature*, vol. 163, no. 4139, pp. 324325, Feb. 1949.

[3] R. E. Collin, *Field Thery of Guided Waves, 2nd Ed.* IEEE Press, New York, 1990.

[4] W. H. Syed and A. Neto, "Front-to-back ratio enhancement of planar printed antennas by means of artificial dielectric layers," *IEEE Trans. Antennas Propag.*, vol. 61, no. 11, pp. 5408-5416, Nov. 2013.

[5] W. H. Syed, G. Fiorentino, D. Cavallo, M. Spirito, P. M. Sarro, and A. Neto, "Design, fabrication and measurement of 0.3 THz on-chip double-slot antenna enhanced by artificial dielectrics," *IEEE Trans. THz Sci. Tech.*, vol. 5, no. 2, pp. 288-298, Mar. 2015.

[6] D. Cavallo, W. H. Syed, and A. Neto, "Closed-form analysis of artificial dielectric layers—Part I: Properties of a single layer under plane-wave incidence," *IEEE Trans. Antennas Propag.*, vol. 62, no. 12, pp. 6256-6264, Dec. 2014.

[7] D. Cavallo, W. H. Syed, and A. Neto, "Closed-form analysis of artificial dielectric layers—Part II: Extension to multiple layers and arbitrary illumination," *IEEE Trans. Antennas Propag.*, vol. 62, no. 12, pp. 6265-6273, Dec. 2014.

[8] S. A. Schelkunoff, "Some equivalence theorems of electromagnetics and their application to radiation problems," *Bell System Tech. J.*, vol. 15, pp. 92-112, 1936.

[9] CST Microwave Studio, CST [Online]. Available: http://www.cst.com/

[10] D. Cohen and R. Shavit, "Bi-anisotropic metamaterials effective constitutive parameters extraction using oblique incidence S-parameters method," *IEEE Trans. Antennas Propag.*, vol. 63, no. 5, pp. 2071-2078, May 2015.